

THE ADSORPTION OF N₂: CHEMISORBED ON Ni(110) AND PHYSISORBED ON Pd(111)

K. HORN

Fritz-Haber Institut der Max-Planck-Gesellschaft, Faradayweg 4-6, D-1000 Berlin, Fed. Rep. of Germany

and

J. DiNARDO, W. EBERHARDT, H.-J. FREUND and E.W. PLUMMER

Department of Physics, University of Pennsylvania, Philadelphia, Pennsylvania 19104-3859, USA

Received 9 September 1981; accepted for publication 2 February 1982

The bonding of molecular N₂ has been investigated with angle resolved photoelectron spectroscopy and inelastic electron scattering. The spectra obtained from N₂ chemisorbed onto a Ni(110) surface are compared to CO chemisorbed onto Ni(110) and to N₂ physisorbed onto Pd(111). The N₂ molecular axis was found to be normal to the crystal surface for the chemisorbed state on Ni(110) and random for the physisorbed state on Pd(111). The N-N and Ni-N₂ stretching frequencies indicate that the N₂ molecule is terminally bonded to a single Ni atom on Ni(110). The binding energies of the two outer σ states and one π state of chemisorbed N₂ were measured, indicating that the bonding of N₂ to a metal surface is different than CO. Both σ states drop in energy compared to the π level due to the fact that both of them are involved in the N₂ substrate bond. The symmetry of the gas phase N₂ molecule is reduced upon adsorption. The consequences of this are seen in the dipole active N-N vibrational mode, the large intensity of the Ni-N₂ vibrational mode and the coupling of the adsorbate $4\sigma(2\sigma_u)$ level to the final state resonance which is forbidden by symmetry in the gas phase. Many electron excitation satellite lines are observed in the valence spectra of both the chemisorbed and physisorbed N₂. The physisorbed satellite lines are nearly identical to those seen in gas phase N₂, while the chemisorbed N₂ spectra has new satellite structure, due to the interaction with the substrate.

1. Introduction

The adsorption of CO on transition metal surfaces has served as the prototype system of molecular adsorption to check new theoretical schemes and experimental techniques. As a consequence, there is a considerable bank of knowledge about the CO-metal bond and how we should interpret the various spectroscopic techniques. In strong contrast, the adsorption of isoelectronic N₂ has been largely neglected, despite the similarities between the two molecules. There exist experimental photoemission data for N₂ adsorbed on

W(100) [1–3], Ni(110) [4] and Ni(100) [5], inelastic electron scattering data for W(100) [6], and infrared reflectance data for Ni(110) [7] and Pt(111) [8]. Bagus and his coworkers have investigated theoretically the bonding of N_2 to a single Ni atom and compared their results with photoemission spectra [5,9,10]. In this work we used angle resolved photoelectron spectroscopy to study the electronic states and bonding symmetry of N_2 chemisorbed on Ni(100) and physisorbed on Pd(111). High resolution inelastic electron scattering was used to measure the vibrational modes of the chemisorbed system.

Fig. 1 shows the wave function contour plots for the valence orbitals of N_2 (left) and CO (right). The N_2 molecule has inversion symmetry, meaning that in the $D_{\infty h}$ symmetry notation each level is labeled with a g (gerade or even) or u (ungerade or odd). This notation is shown in parentheses, while the $C_{\infty v}$ notation of CO is used to label the N_2 orbitals. Even though N_2 and CO are

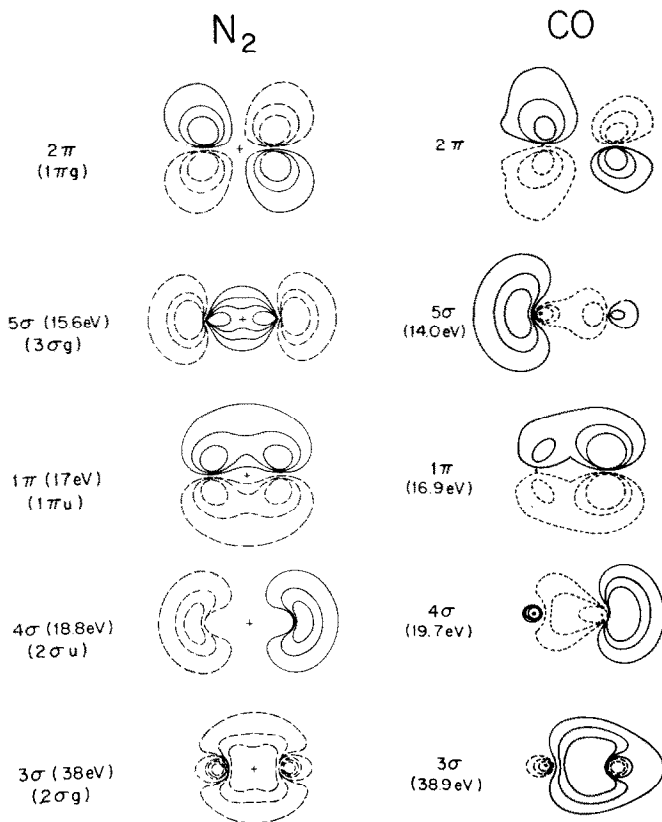


Fig. 1. Wave functions for CO [11] and N_2 [12], the binding energies are given in the parentheses. The contours have values of 0.3, 0.2 and 0.1. The carbon end of the CO molecule is to the left.

isoelectronic, most of the individual orbitals are quite different. The CO 4σ and 5σ orbitals are lone pair type orbitals on the oxygen and carbon, respectively, while the N₂ 4σ and 5σ orbitals both have about the same spatial extent along the molecular axis and are by definition democratically shared by both nitrogen atoms. Likewise the unoccupied CO 2π has much more weight toward the carbon end, where the metal atom will bond, than does the equivalent orbital in N₂.

Qualitatively, the bonding of CO to a transition metal is understood [11,13,14,15]. The lone pair orbital (5σ) is the primary orbital involved in the bond. The standard words are that there is σ donation from the CO 5σ to the metal and a small amount of metal dπ back bonding into the CO 2π level. The other valence levels are only slightly affected by the bond. This picture has two direct consequences: (1) the bonding CO 5σ level will drop in energy relative to the CO 1π and 4σ levels. Since the 1π and 4σ are not changed upon bonding, their energy spacing should stay fixed (compared to the gas phase) and (2) the partial occupancy of the CO 2π orbital weakens the CO bond, causing the CO stretching frequency to drop in energy compared to gas phase CO. Fig. 1 shows that the CO 2π orbital is antibonding with respect to CO.

The bonding of N₂ to a metal atom must be different from the bonding of CO to a metal atom. The adsorption energy of N₂ on Ni(110) is only 0.36 eV [7], while CO adsorption energies on Ni exceeds 1 eV. The reason for the difference can be seen in fig. 1, for example the valence σ orbits (5σ and 4σ) have approximately the same spatial extent along the molecular axis. This means that if the N₂ molecule is terminally bonded to a metal atom, then the metal electrons will equally overlap both σ states. This interaction with a metal atom will break the symmetry of the N₂ molecule, allowing the 2σ_u and 3σ_g N₂ states to mix, forming two new σ states which will look more like the CO lone pair σ states [5,10]. The degree of mixing of the σ states will depend upon the strength of the N₂-metal bond. This qualitative picture of the N₂-metal bond predicts several spectroscopically observable features, due to the reduction in symmetry [10]:

- (1) Both of the valence σ orbitals should be shifted compared to gas phase N₂, due to bonding.
- (2) The N-N stretching vibrational mode should be infrared active.
- (3) The two nitrogen atoms should be inequivalent producing different core level binding energies [1,16].

Grunze et al. [7] observed the infrared active N-N stretching mode of N₂ adsorbed on Ni(110). The relatively large infrared absorption by the N₂ stretching mode implies that the molecular axis of the N₂ molecule is nearly normal to the surface. When N₂ was adsorbed at 127 K, the N₂ mode appeared at 2194 cm⁻¹ at low coverage and shifted to 2189 cm⁻¹ at higher coverages. The work function increased by 0.1 eV. Adsorption at 81 K resulted in a shift of the N-N stretching mode to smaller wave numbers as the coverage was increased to where the work function change was 0.1 eV, then an increase back

to 2194 cm^{-1} as the coverage was increased beyond that possible at 127 K. The work function change for this 81 K saturated layer went back to nearly zero. Obviously the coverage dependent shifts are due to N_2-N_2 dipole interactions and to changes in the bond energy with coverage. Grunze et al. [7] measured a binding energy of 0.36 eV at low coverages, which decreased to ~ 0.28 eV at high coverages for a crystal at 81 K.

There has been no previously reported photoemission data for N_2 adsorbed on Ni(110), but Brundle has published data for N_2 adsorbed on Ni(100) [5,16]. The angle integrated valence band spectrum shows two new peaks caused by N_2 adsorption. The most intense and narrowest peak occurs at an energy 8 eV below the Fermi energy, while the broad weak peak is ~ 12 eV below the Fermi energy [5]. Brundle identified these peaks by comparing the results for CO on Ni(100), i.e. the -8 eV peak is due to the 5σ and 1π levels of N_2 and the -12 eV peak is due to the 4σ level of N_2 . Bagus and Hermann's calculations confirmed this assignment [5,10]. The N_{1s} core level spectra show two broad peaks, but the two peaks are not a direct consequence of inequivalent N atoms. Hermann and Bagus [9] have shown that the two peaked core level spectrum is caused by shake-up.

The only other published photoemission data for N_2 adsorption is for a W(110) substrate [3,16]. N_2 does not dissociatively adsorb on W(110). The angle integrated valence band spectra showed a narrow (~ 1 eV) peak at -7.4 eV and a broad band near -12 eV. The position and shape of the -7.4 eV N_2 induced level did not change with collection angle or photon energy. The broad -12 eV band did show considerable change with both collection angle and photon energy. At certain collection geometries this band clearly appeared to be composed of multiple peaks. Umbach et al. [3] used the measured angular variations of these peaks and compared them to a theoretical calculation to determine that N_2 was bound standing straight up on W(110). The theoretically calculated angular intensity for the -12 eV peak, which they assume to be the 4σ level, did not agree with experimental data as well as the calculations for the -7.4 eV peak (1π and 5σ). This discrepancy, according to the authors of this paper, may be due to satellite lines (shake-up) from the 5σ and 1π level at -7.4 eV appearing near the -12 eV peak. We will show that this broad spectra feature in the adsorbed N_2 spectra near -12 eV is due to many satellite lines. Fuggle et al. [1,2,16] also observed the inequivalent N_{1s} core level binding energies for N_2 on W(110).

Experimentally [17] and theoretically [18] it is known that there is a resonant state of σ_u symmetry in the continuum of N_2 . This same resonant state in the continuum has been seen in gas phase CO and N_2 [17], adsorbed CO [19] and transition metal carbonyls [20]. The gas phase partial photoionization cross sections for N_2 differ from CO because of the N_2 inversion symmetry. A σ symmetry initial state can be excited into the σ resonant state only by the component of the electromagnetic field parallel to the molecular axis. The vector potential is odd with respect to the inversion operation, so the

photoionization matrix element from σ_u to σ_u is identically zero. Therefore, the cross section as a function of photon energy for photoionization from the $2\sigma_u(4\sigma)$ energy level of gas phase N₂ shows no resonant behavior, while the $3\sigma_g(5\sigma)$ cross section shows a large resonance at $\hbar\omega = 28$ eV or at ~ 12 eV kinetic energy. If the inversion symmetry is destroyed when N₂ is adsorbed the resonance in the 4σ cross section should be observable [16].

2. Experimental

The photoemission system used in our study has been described in detail before [21]. It consists of a vacuum chamber with a moveable electron energy analyzer which is rotatable about two orthogonal axes. As a light source we used synchrotron radiation from the 240 MeV storage ring of the Synchrotron Radiation Center of the University of Wisconsin–Madison. The radiation was dispersed by a toroidal grating monochromator equipped with two holographically ruled gratings [22]. The combined resolution of the analyzer and monochromator was kept at ~ 0.2 eV during most of these measurements. The photon flux was measured during recording of the spectra by the photocurrent emitted from a tungsten mesh (84% transmission) which was situated in the light beam. The sample was a Ni(110) single crystal cut and polished to within 1° of the desired orientation. It was cleaned in situ by cycles of argon ion bombardment and annealing to 750°C. The crystal was mounted on a crystal holder which allowed cooling to 90 K by using liquid nitrogen, or even lower when liquid helium was used, while maintaining full azimuthal rotation about the crystal normal. After the final heating, the crystal cooled to 100 K within 5 min. Since N₂ has a low adsorption energy on Ni(110), ca. 0.36 eV [7], and is readily displaced by strongly adsorbed CO, fast cooling was an important prerequisite to our experiment. During gas exposure, the ion pump was valved off in order to prohibit contamination of the nitrogen gas through backstreaming from the pump.

The Pd(111) crystal was loaned to us by P.O. Nilsson. The crystal which had previously been extensively cleaned was cleaned in our chamber by repeated sputter annealing cycles.

An angle resolved electron loss spectrometer operating at 12–16 meV resolution was used for the vibrational studies. We used 180° spherical elements to disperse the electrons in the monochromator and analyzer. The angular resolution was $\pm 0.8^\circ$ and the angle of incidence was varied between 42° and 65° with respect to the crystal normal. The electron energy analyzer rotated in a plane so that the angular dependence of the scattering intensity could be measured. This system was pumped by an ion pump and a liquid nitrogen cooled Ti sublimator giving background pressures in the 10^{-11} Torr range. Single crystal samples were cooled to copper braid running from a

liquid nitrogen reservoir. The lowest temperature attainable with this cooling state was ~ 125 K.

3. Experimental results

3.1. Inelastic electron scattering

Fig. 2 shows the inelastic electron scattering spectra for CO and N_2 adsorbed on Ni(110) at 130 K. The CO spectrum at the top is presented for comparison to N_2 . There are two losses observed in both the CO and N_2 spectra. For adsorbed CO, these vibrational states are at 248 and 51 meV. The 248 meV mode is the C–O stretch and the 51 meV mode is the Ni–CO stretch. The energy width of the 248 meV loss is wider than the elastically scattered peak, presumably because there are several binding sites with different stretching frequencies contributing to the spectrum [23]. We cannot resolve these separate peaks. The CO stretching frequency is shifted to lower energy compared to the gas phase value of 265 meV. It is even lower than the value of 255 meV observed for $Ni(CO)_4$ [24], probably indicating that some of the CO molecules are bridge bonded [23]. This shift in the C–O stretching energy is usually attributed to 2π backbonding. The 51 meV Ni–CO stretch is close to the value of 52 meV observed in $Ni(CO)_4$ [24].

Fig. 2b shows that there are only two major losses for adsorbed N_2 . The N–N stretch at 271 meV and the NN–Ni stretch at 40 meV. The weak band near 72 meV is most likely due to dissociated N_2 [6,7]. The vibrational energies for adsorbed N_2 can be compared to transition metal–dinitrogen complexes to obtain a preliminary determination of the bonding configuration. The energy of the N–N stretch is shifted upon chemisorption by 17 meV from the gas phase N_2 value of 288 meV. Folkesson's data for Ru and Os linearly bonded dinitrogen complexes give a range of 248 to 265 meV for the N–N stretch and 60 to 64 meV for the metal– N_2 stretch [25]. The N–N stretch for doubly bonded N_2 or bridge bonded N_2 is in the energy range of 190 to 205 meV [26]. In addition, Klotzbucher and Ozin have measured the vibrational energies of $Ni(N_2)_x$ clusters in an argon matrix [27]. They find that the N–N stretch energy increases from 258.8 to 296.4 meV and the NN–Ni stretch decreases from 57.7 to 34.9 meV as x goes from 1 to 4. The N_2 molecule is terminally bonded in all cases. The vibrational energies for the saturated complex $Ni(N_2)_4$ are close to those for adsorbed N_2 : 269 meV for the N–N stretch and 35 meV for the NN–Ni stretch. Therefore, we would conclude from this comparison to transition metal–dinitrogen complexes that the adsorbed N_2 still has a triple N–N bond and is bonded to a single Ni atom in a linear arrangement. The last part of this conclusion must be taken with appropriate skepticism, since there may be forms of bridge or trigonally bonded N_2 on a surface that are not found in finite clusters.

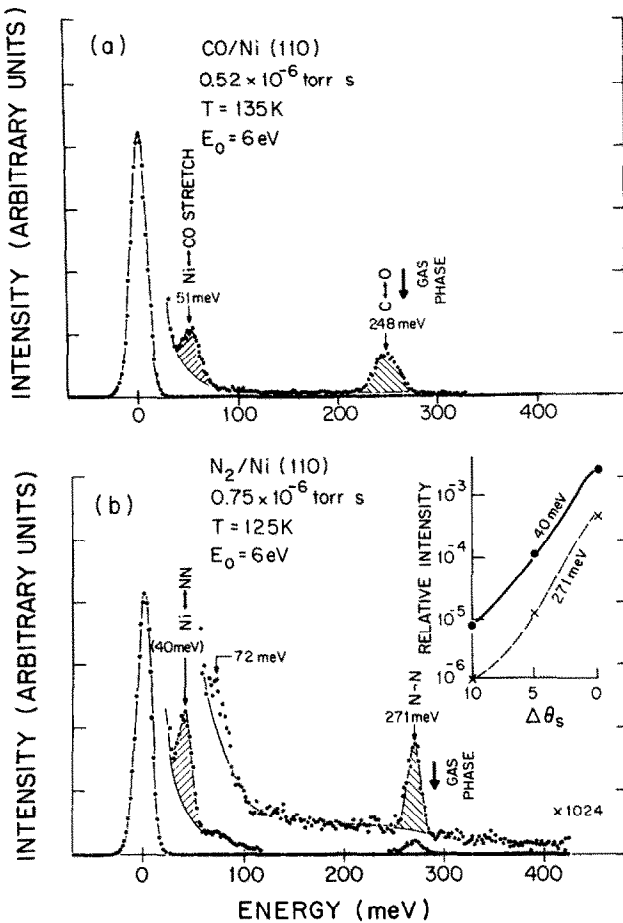


Fig. 2. Inelastic electron scattering spectra for CO and N_2 adsorbed on Ni(110) at ~ 125 K: (a) CO; (b) N_2 . Both curves are for collection in the specular direction with a 6 eV incident beam. The insert in (b) shows the angular dependence of the intensity of the N_2 modes as the collection angle is moved from specular ($\Delta\theta_s = 0$ at specular). The intensity scale of the insert is relative to the elastic beam at $\Delta\theta_s = 0^\circ$.

We will present data both from inelastic electron scattering and photoemission that will substantiate the bonding configuration proposed in the previous paragraph, i.e. the N_2 molecular axis is perpendicular to the surface. The first experimental evidence for this bonding configuration came from the infrared data of Grunze et al. [7]. They observed a very intense absorption band from the N-N stretch when N_2 was adsorbed onto Ni(110). This means that the inversion symmetry of gas phase Ni is removed upon adsorption, so that the N-N stretch is infrared active, and more importantly that the molecular axis

of the N₂ is nearly normal to the surface. If the molecular axis was parallel to the surface there could be a dipole active mode but it would be very weak. The inelastic electron scattering data shown in fig. 2 allow us to calculate the strength of the infrared modes for adsorbed CO and N₂. Dipole active vibrational modes can easily be identified in electron scattering by measuring the intensity versus scattering angle away from the specular direction ($\Delta\theta_s$). The few points shown in the insert of fig. 2b prove that both modes are infrared active because the scattering takes place via the long range dynamic dipole. The strength of the dynamic dipole is characterized by an effective charge e^* [28].

If θ_{N_2} and θ_{CO} are the fractional coverages of N₂ and CO respectively, then the effective charge e^* is

$$e^* = 0.223e/\sqrt{\theta_{N_2}} \quad \text{for 40 meV N}_2 \text{ mode,} \quad (1a)$$

$$e^* = 0.321e/\sqrt{\theta_{N_2}} \quad \text{for 271 meV N}_2 \text{ mode,} \quad (1b)$$

$$e^* = 0.17e/\sqrt{\theta_{CO}} \quad \text{for 51 meV CO mode,} \quad (1c)$$

$$e^* = 0.51e/\sqrt{\theta_{CO}} \quad \text{for 248 meV CO mode.} \quad (1d)$$

The coverage of CO in fig. 2 is greater than the N₂ coverage and is probably nearly a monolayer. A comparison of our N₂ exposure and crystal temperature with the data of Grunze et al. [7] gives a N₂ coverage of $\lesssim 0.5$ of a monolayer. With this coverage eqs. (1a) and (1b) give:

$$e^*(N-N) \gtrsim 0.45e, \quad (2a)$$

$$e^*(Ni-NN) \gtrsim 0.31e. \quad (2b)$$

The e^* for the N–N stretch is appreciable compared to those obtained for adsorbed CO, which are in the range of 0.6 to 0.7 [29]. The N₂ molecule has lost its inversion symmetry and the strength of this dynamic dipole indicates that the molecular axis is nearly perpendicular to the surface plane. The surprising feature of fig. 2 and eq. (2) is the large absolute strength of the NN–metal stretch compared to either the N–N stretch or the CO–metal stretch. This must also be a consequence of the symmetry breaking in N₂ as it approaches the surface. When a CO or N₂ molecule moves back and forth with respect to the metal surface, the amount of charge transfer to or from the molecule changes, creating a dynamic dipole. There is an additional effect in N₂, caused by the reduction in symmetry. As the N₂ molecule vibrates with respect to the metal surface, the degree of mixing of the N₂ $2\sigma_u(4\sigma)$ and $3\sigma_g(5\sigma)$ states changes, inducing a contribution to the dynamic dipole moment not present in CO.

This behavior of the intensity of the NN–metal stretch compared to the N–N stretch has been observed for transition metal–dinitrogen complexes. Folkesson's data [25] for ruthenium and osmium linearly bonded complexes

give a ratio of $e^*(\text{metal-N}_2)/e^*(\text{N-N})$ in the range of 0.8 to 1.3, while our ratio for adsorbed N_2 is 0.7. The equivalent ratio for adsorbed CO is $\sim < 0.2$.

3.2. Photoemission

Fig. 3 compares the normal emission photoelectron spectra of adsorbed CO (a) and N_2 (b). The two major peaks in the CO spectrum at -11.3 and -8.4 eV are due to the CO 4σ and 5σ states, respectively. The dotted curve shows the CO 1π level at -6.5 eV, which can be identified using a different measurement geometry [30]. The shift in the levels from their gas phase binding energies is shown at the top. When CO is adsorbed at room temperature onto Ni(110), the positions of the peaks are different from that shown in

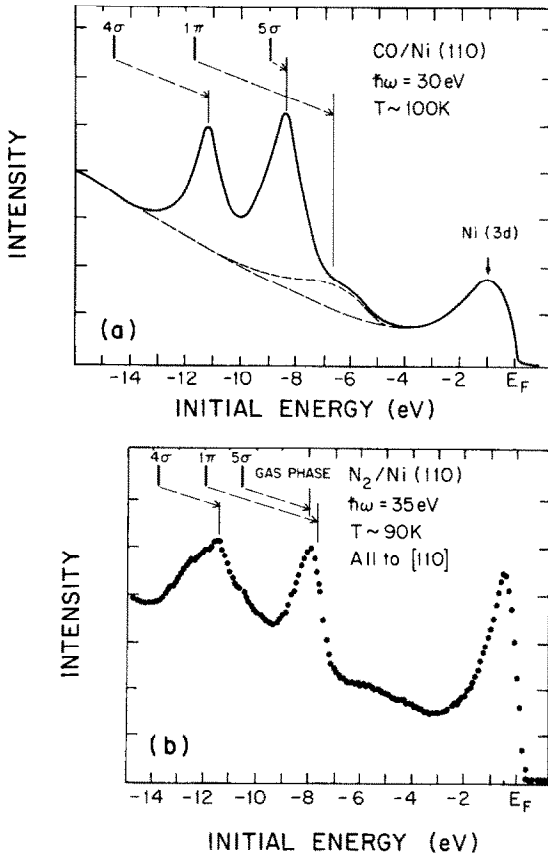


Fig. 3. Photoelectron spectra of CO and N_2 adsorbed on Ni(110) at ~ 100 K: (a) CO; (b) N_2 . Both spectra are for p-polarized light and normal collection. The CO exposure was 1 L and the N_2 exposure 5 L (1 L = 1×10^{-6} Torr s).

fig. 2a. The 4σ is at -10.8 eV, the 5σ at -8.0 eV and the 1π at -7.7 eV [32]. The shift of the levels in the 100 K spectrum compared to the room temperature spectrum is caused by more CO adsorbing producing two effects: (1) the CO bond energy decreases and (2) the CO-CO interaction induces dispersion in the CO levels [33]. The 1π band is antibonding at $\bar{\Gamma}$ (normal emission) and is consequently shifted towards the Fermi energy due to the CO-CO interaction. We have measured over 1 eV dispersion in this 1π level for the 100 K saturated layer.

The picture of the surface-CO bond in the low coverage regime where dispersion is not important is quite simple. The 1π and 4σ levels, which undergo only minor perturbations upon adsorption, are shifted to lower binding energy by approximately 4 eV. This is caused by screening of the photoinduced hole and is usually referred to as relaxation. This shift is seen whenever CO is bound to a metal and is ~ 2 eV for single metal carbonyls [34]. The CO 5σ level forms a bond with the Ni and drops in energy (increased binding energy) by approximately 3 eV. The combination of the upward relaxation shift and the downward bonding shift leaves the 5σ bonding orbital nearly degenerate with the 1π adsorbate level. This qualitative picture is correct for all chemisorbed CO systems where dispersion is not of importance [32] and for all stable carbonyls [34]. Since the 1π and 4σ are basically not involved in the bonding, their relative energy spacing stays nearly constant [32], increasing by only 0.3 eV for room temperature adsorption of CO on Ni(110). This increase may result from antibonding CO 2π character mixed into the CO 1π orbital of the bound complex.

Fig. 3b shows the photoelectron spectrum of N_2 adsorbed onto Ni(110) at 90 K. Qualitatively, the spectrum looks very similar to the CO spectrum, two peaks at ~ -12 and ~ -8 eV. The vertical lines show the identification of the σ and π levels using angle resolved detection, which will be discussed later. As in the case of CO adsorption, the 5σ and 1π are nearly degenerate, but the relative shifts of the levels from the gas phase N_2 molecule are quite different from CO. The 1π level shifts up towards the Fermi energy by 4 eV. Since the 1π is not expected to participate in the bond, this shift is predominantly due to a final state relation shift. The magnitude of the N_2 1π shift is similar to the shift of the CO 1π level. The behavior of the two N_2 σ states is quite different from that of the σ states of chemisorbed CO. For CO, the energy separation of the σ states decreased by approximately 3 eV with the 4σ to 1π spacing remaining basically constant. For adsorbed N_2 on Ni(110), the 4σ to 5σ spacing increases by 0.5 eV and the 4σ to 1π spacing increases by ~ 2 eV. The simplest explanation of these results is that both the N_2 4σ and 5σ levels are bonding to the Ni, dropping in initial state energy [10,35]. This makes the N_2 -Ni bond quite different from the CO-Ni bond.

There is another conspicuous difference between the N_2 and CO spectra. The -12 eV peak in the N_2 spectrum is very broad and looks like a combination of multi-peaks. This behavior was observed by Umbach et al. [3] in their data for

N_2 on W(110). We will show that this is due to shake-up processes in the valence band excitation [15]. Shake-up refers to multi-electron excitations.

The bonding orientation of the molecular axis as well as the assignment of the different symmetry levels shown in fig. 3b for adsorbed Ni was determined using selected angles of collection and light polarization. A typical set of spectra are shown in fig. 4. Curve a is a normal emission spectrum with p polarized light. All of the N_2 levels should be excited in this configuration, independent of the N_2 molecular orientation. Curves b and c are for s polarized light with a collection angle of 30° with respect to the normal. In (b) the collection is in the plane defined by the surface normal and the polarization vector while the data in curve (c) are taken in a plane perpendicular to the polarization vector. If the N_2 molecule is standing upright on the surface, curve b should show the σ states and the even component of the degenerate π state and only the odd π state should be excited in curve c. Qualitatively, the spectra behave properly in that the 8 and 12 eV peaks, which should be the σ states, are substantially reduced in curve c compared to curve b. This indicates that the N_2 axis is sticking up from the surface. We can not quantify this statement as Allyn et al. [19] did for CO on Ni(100), because there are several peaks in the spectra region of the 4σ state. The shape of the 12 eV peak is different in each curve of fig. 4.

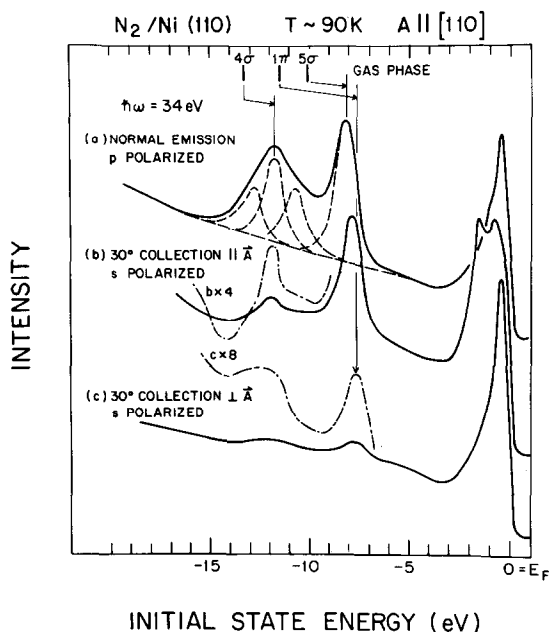


Fig. 4. Angle resolved photoelectron spectra of N_2 adsorbed on Ni(110) at 90 K. The exposure was 1 L.

The multi-peak structure in the region of the 4σ level (-12 eV) is due to shake-up on the valence orbitals. Curve a shows a three peak decomposition of this wide band using peak positions seen in other spectra – like (b) – and a peak width equal to the 5σ width (~ 1.1 eV). The problem is to ascertain which peak is the primary 4σ peak and which are multi-electron excitations. If the mixture of the single particle states is too large, this question may be meaningless. What can be determined from curves b and c is, which parts of the spectra have even (b) or odd (c) symmetry with respect to the plane defined by the surface normal and the collector.

We rule out the possibility of multiple binding sites being the origin of the multiple peaked structure in the 4σ region. Our vibrational studies showed only one N–N stretching mode and the infrared data of Grunze et al. [7] showed only one N–N mode for all coverages [7]. The infrared study showed a 0.6 meV shift in the N–N stretch energy between saturation exposure at 81 K compared to 127 K, caused by the increased coverage of N_2 at the lower temperature. Our inelastic electron scattering data was taken at 125 K where the coverage was in the low coverage regime of the infrared experiment, while the substrate temperature in the photoemission experiment was low enough to populate the higher coverage regime seen in the infrared experiments. We observed no noticeable changes in the line shape as a function of exposure in the photoemission experiments. The photoemission curve shown in fig. 3b is for 5 L exposure, which according to Grunze et al. [7] is high enough to populate the high coverage regime, while the spectrum in fig. 4 is for 1 L and should be in the low coverage regime. There is no measurable difference in these two spectra.

An unambiguous determination of the direction of the molecular axis was not possible using angle resolved data shown in fig. 4, because of the complexities introduced by the satellite lines in the region of the 4σ energy level. We searched for another system where the N_2 was bound with a random orientation to compare to the Ni(110) data. N_2 only physisorbs onto Pd(111) as judged by the photoelectron spectra which looks like gas phase N_2 and by the low desorption temperature. Fig. 5 shows the same set of angle resolved spectra shown in fig. 4, except for physisorbed N_2 on Pd(111) at 45 K. There are three peaks in all of the spectra which are labeled at the bottom using the gas phase notation. The three peaks have the relative intensities seen in the gas phase [17] (15%, 55% and 30%) and their initial state energies of -11.9 , -10.3 and -8.7 eV are just rigidly shifted upward by approximately 1.3 eV compared to gas phase N_2 . The three peaks appeared in all measurement geometries with the same relative intensity. This proves that the molecular orientation of physisorbed N_2 on Pd(111) is nearly random. In spite of problems with the shake-up, fig. 4 can be used in comparison with fig. 5 to support our conclusion that the orientation of N_2 on Ni(110) is basically normal to the surface.

Several other studies on different substrates have concluded that N_2 chemisorbs to the surface standing straight up. Umbach et al. [3] came to this

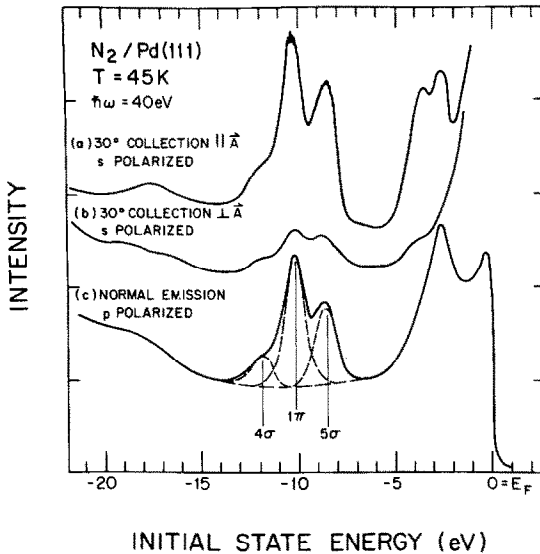


Fig. 5. Angle resolved photoelectron spectra of N_2 adsorbed on Pd(111) at 45 K. These curves are for an exposure of 2×10^{-6} Torr s.

conclusion for N_2 on W(110) from comparisons of experimental and theoretical photoemission angular profiles. X-ray core level data has been used to argue that N_2 is bound vertically on W(110) [16]. In all of these measurements, the uncertainty upon the possible bending of the N_2 axis with respect to the surface can not be determined.

When the N_2 molecule is standing straight up on the surface, we can simply apply symmetry rules to measure the binding energy of the 1π level. The peaks in curve c of fig. 4 are due to odd initial states [30,32]. The largest peak in curve c at -7.8 eV is the 1π level, the large peak in curve b at -8.0 eV is a composite of the 1π and 5σ levels. Curve b shows a relatively narrow peak at -11.8 eV which we believe is the major component of the 4σ level. The 5σ level seen in normal emission (curve c) is at 8.1 eV and appears to shift to -7.9 eV in curve b. Either there is dispersion in the 5σ level, or the 1π level in curve b is intense enough to shift the apparant peak position. Table 1 lists the experimental and theoretical binding energies of gas phase N_2 and N_2 bound to a transition metal. The binding energies of adsorbed N_2 are measured from the Fermi energy, while the gas phase N_2 data is referred to the vacuum level. The Δ 's in table 1 are the differences in binding energy between the gas phase and the adsorbed molecule using the values of the clean surface work function to refer the Fermi energy to the vacuum level [36,37]. The work function increases by ~ 1 eV upon CO adsorption [38] and 0.1 eV for N_2 adsorption [7]. We will discuss the theoretical calculations in a later section.

Table 1
Binding energy of N₂-metal systems

Theory	System	Binding energy ^a (eV)								Comments	
		5σ	Δ _{5σ}	1π	Δ _{1π}	4σ	Δ _{4σ}	3σ	Δ _{3σ}		
	N ₂	15.6		17		18.8		38			
	N ₂ on Pd(111)	8.7	1.3	10.3	1.1	11.9	1.3	31.3	1.1		
	N ₂ on Ni(110)	8.1	2.5	7.8	4.2	11.8	2.0				
	N ₂	15.89		15.32		20.18		37.7			<i>d</i> (Ni-N) = 1.92 Å
SCF-HF [10]	NiN ₂	16.46	-0.57	16.32	-1.00	21.58	-1.40	38.36	+0.7		<i>d</i> (N-N) = 1.1 Å
SCF-HF [10]	N ₂	15.5		17.0		19.4					<i>d</i> (Ni-N) = 1.83 Å
SCF X _α [35]	N ₂	17	-1.5	15.6	1.4	20.4	-1.0				<i>d</i> (N-N) = 1.1 Å
SCF X _α [35]	N ₂	17.5		21.4		23.4		45.6			<i>d</i> (Ni-N) = 1.82 Å
SCF-MO-CNDO [15]	N ₂	15.4	+2.1	17.9	3.5	21.4	2.0	47.2	-1.6		<i>d</i> (N-N) = 1.1 Å
SCF-MO-CNDO [15]	NiN ₂										

^a The N₂ and cluster calculation binding energies are with respect to the vacuum level. The adsorbate binding energies are with respect to the Fermi energy. The notation Δⁱ designates the energy difference, i.e. Δ = *E*(gas) - *E*(complex). When comparing experimental results, the clean metal work function is used *E*(complex) = *E*_{binding} + φ, with φ = 5.0 eV for Ni(110) [36] and 5.6 eV for Pd(111) [37].

The photoionization cross section from the 4σ level of adsorbed N₂ should exhibit a resonant behavior, since the symmetry has been reduced. Fig. 6 shows a series of photoelectron spectra of N₂ on Ni(110) for photon energies in the range $22 \text{ eV} < \hbar\omega < 40 \text{ eV}$. All of the spectra were recorded at normal electron emission and 50° angle of incidence. Both nitrogen-induced peaks exhibit intensity variations with photon energy, most strongly the peak at 8.1 eV. The spectra were normalized with respect to the photon flux. The peak area is shown as a function of photon energy in fig. 7. The $3\sigma_g$ or 5σ level with a binding energy of 8.1 eV exhibits a clear resonant behavior, with a maximum at $\sim 28 \text{ eV}$. This should be compared to the calculated value shown for gas phase N₂ shown by the solid line [18] and to the experimental resonance which is observed at the same position in photon energy for gas phase and adsorbed N₂. The kinetic energy position of the resonance is 2 eV lower in adsorbed N₂ due to the relaxation energy of the 5σ energy level. The integrated area of the 12 eV binding energy peak in fig. 6 also shows a resonant behavior at $\hbar\omega \cong 31 \text{ eV}$. The behavior of the two cross sections is very similar to what Allyn observed for CO on Ni surfaces [19,32]. There are quantitative differences between the cross sections of chemisorbed CO and N₂. Compared to the 5σ cross section, the 4σ cross section is smaller for N₂ than for CO.

The solid lines in fig. 7 are the angle integrated gas phase calculations of Davenport [18]. They show the resonance in the $5\sigma(3\sigma_g)$ and non-resonant behavior of the $4\sigma(2\sigma_u)$ caused by the symmetry restriction in N₂. The presence of the resonance in the cross section of the 12 eV peak would indicate that we have another measure of the symmetry reduction in adsorbed N₂. The problem is that we know there are several peaks contained in this broad spectral region (see figs. 3 and 4). In fact, fig. 6 shows that the shape of this peak changes with photon energy. You can see that near $\hbar\omega = 26 \text{ eV}$, the peak

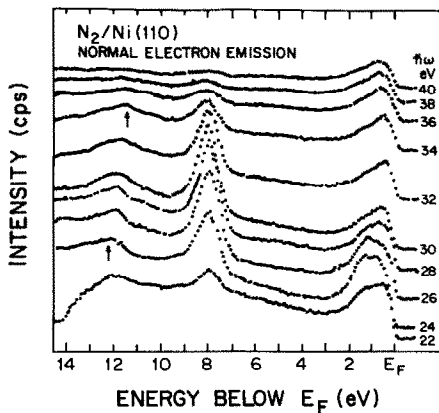


Fig. 6. Photoelectron spectra of N₂/Ni(110) recorded with different photon energies as indicated. All spectra were taken at normal electron emission. Photon angle of incidence 50° .

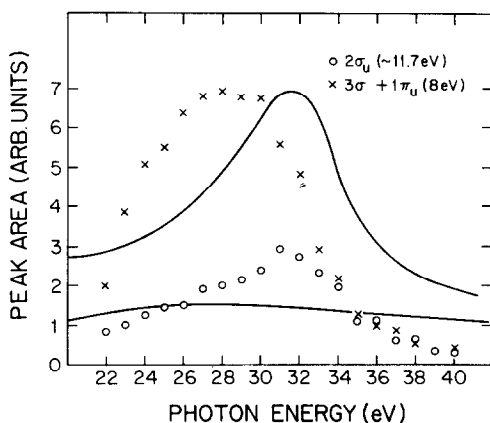


Fig. 7. Intensity of peaks in spectra of fig. 6 as a function of photon energy. The solid lines are calculated values for gas phase N_2 [18].

position is around 12 eV, while at $\hbar\omega = 34$ eV it appears to have shifted to ~ 11.5 eV. We have subtracted a smooth background and expanded a few spectra in fig. 8 to illustrate this effect. The 12 eV peak broadens and shifts as $\hbar\omega$ increases from 25 to 33 eV. The shape and position of the 8 eV peak are independent of photon energy.

This variation in peak position and line shape have been observed before for N_2 adsorbed onto W(110) [3]. In this case, as the photon energy increased the peak position moved away from E_F , in contrast to our data on Ni(110). The explanation for this behavior is that there are a multitude of shake-up peaks in the general region of the 12 eV peak [15]. They have slightly different photon energy dependent cross sections causing the peak position and shape to change with photon energy.

We have shown in fig. 4b that there was a narrow peak at a binding energy of 11.8 eV which we tentatively assigned as the major component of the 4σ level. If this is the 4σ level, then the peak position of the broad 12 eV peak should be near 11.8 eV when the 4σ state goes through the resonance. Fig. 9 shows a plot of the peak position of the -12 eV peak as a function of photon energy. It shows what can be qualitatively seen on fig. 6. The peak moves to lower binding energy as $\hbar\omega$ increases. The important observation is that at $\hbar\omega = 32$ eV the binding energy is ~ 11.8 eV. This is a confirmation that our original assignment of the 4σ state was correct and that the 4σ state does exhibit a resonant behavior.

Another fact emerging from fig. 8 is that there is extra emission in the region between the two peaks around 10–11 eV. Since the 4σ peak of CO is situated at 10.8 eV below E_F on Ni(110), we first thought that the different half-widths and the structure at 10–11 eV were caused by CO co-adsorbed with N_2 either

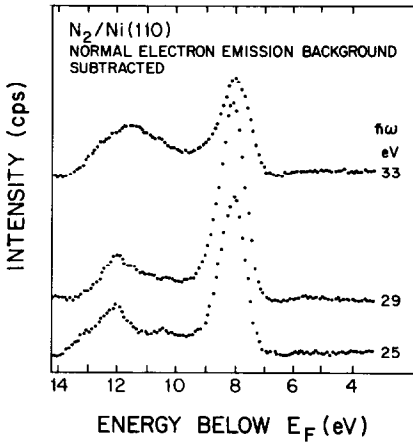


Fig. 8. Comparison of three spectra ($h\omega = 25, 29, 33$ eV) from fig. 6, energy scale expanded.

during the gas exposure or during the recording of the spectra. The following procedure was therefore adopted after each experiment: the crystal was briefly heated to 150 K in order to desorb all N_2 , and another photoelectron spectrum was recorded at $h\omega = 35$ eV. At this energy, the 4σ peak of CO is near an intensity maximum [19,32]. After some changes in the exposure procedure, no peaks due to CO (which only desorbs above ~ 450 K) were observed. It is unlikely that other contaminants, e.g., water, caused the change in appearance of the peak at ~ 12 eV below E_F .

We conclude from our data, both photoemission and inelastic electron scattering, that the broad multi-peaked spectral region near 12 eV binding

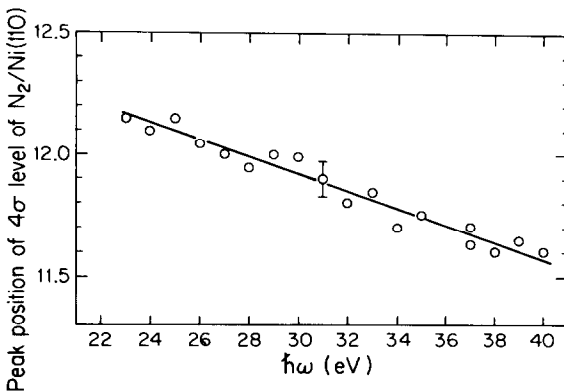


Fig. 9. Peak position of the ~ 12 eV peak in fig. 6 as a function of photon energy.

energy is not a consequence of multiple N_2 binding sites or co-adsorbed CO. It is an inherent characteristic of the adsorbed N_2 photoelectron spectra, and must be due to shake-up satellite lines on the valence excitations. These satellite lines are common in the transition metal complexes like the carbonyls [34], but CO adsorbed on Cu is the only clear example for shake-up on the outer valence levels of an adsorbed molecule [39].

4. Discussion

4.1. Bonding of N_2

First consider physisorbed N_2 on Pd(111). The three N_2 valence levels of physisorbed N_2 shift upward by 1.3 eV, which is the relaxation energy. A condensed film of N_2 exhibits a 0.3 eV relaxation due to the polarizability of the condensed N_2 [40], so approximately 1 eV of the relaxation in physisorbed N_2 is due to the response of the Pd metal to the hole created by adsorption of the photon. There is very little, if any, differential shift of the N_2 levels, i.e. there is no chemical bond.

The electronic energy levels of N_2 chemisorbed onto Ni(110) exhibit large differential as well as absolute shifts. Assume for the moment that the 1π orbital is unperturbed by bonding to the substrate so that we can use it as a reference level. The 5σ shifts down (higher binding energy) by 1.7 eV compared to the 1π . This causes the ordering of the 1π and 5σ to be reversed in chemisorbed N_2 compared to the gas phase N_2 . The 4σ level shifts downward with respect to the 1π level due to bonding by 2.2 eV. These numbers should be compared to the 3.2 eV downward shift of the CO 5σ compared to the CO 1π and the small 0.3 eV shift of the CO 4σ with respect to the 1π . This preliminary analysis of the data is consistent with a model where both N_2 σ orbitals are bonded to the Ni atom, dropping in initial state energy with respect to the 1π orbital [10]. In CO the only major initial state shift is in the CO 5σ level due to metal-CO σ bonding.

There were two implicit assumptions in the previous discussion. The first is that the 1π level can be used as a reference. This is probably correct within a few tenths of an eV. The CO $4\sigma-1\pi$ energy spacing changes upon adsorption by $\lesssim 0.3$ eV which gives an indication of the possible error. The second assumption is that the final state relaxation energy is nearly the same for all of the valence orbitals. Separating an initial state shift from a final state (relaxation) shift is in general only possible theoretically [41]; therefore different theoretical approaches will give different answers. The Hartree-Fock calculation of Bagus and Hermann predicts a larger relaxation energy for the 5σ orbital of coordinated CO and N_2 than for either the 4σ or 1π orbital [10]. This is a differential of 0.3 eV for CO and ~ 0.6 eV for N_2 . Therefore, the ~ 1.7 eV experimentally observed shift of the N_2 5σ relative to the N_2 1π is not all due

to a bonding shift, only ~ 1.1 eV is an initial state shift. In contrast, X_α scattered wave calculations do not show any change in the energy level spacings between the ground state orbital energies and the transition state energies [35]. The transition state energy in the X_α theory is the actual binding energy, while the orbital energy for the ground state is not the same as the Hartree–Fock orbital energy.

In tables 1 and 2, we compare our photoemission data for N₂ adsorbed on Ni(110) with three different calculations of the linear Ni–N₂ cluster. The first theoretical calculation uses the well defined Hartree–Fock (HF) procedure where the binding energies are calculated by taking the total energy difference between the ionic state (specific hole state) and the ground state of the neutral (called Δ SCF) [10]. By definition, what is left out of this calculation is the correlation energy. The second theoretical calculation shown in table 1 uses the X_α scattered wave approach. The exchange–correlation potential is treated as a local potential, with a parameter α characterizing each atom. The parameter α is tabulated by comparing X_α calculations for atoms with HF calculations. The binding energy is calculated using the transition state energy, which amounts to calculating the orbital energy with the level to be ionized containing only $\frac{1}{2}$ of an electron. The final theoretical scheme listed in table 1 is a many-body Green function technique called SCF–MO–CNDO [15]. It is of a more semiempirical nature than the other two procedures, since it uses CNDO single particle wave functions fit to HF calculated wave functions as a starting point. The many-particle effects are calculated using a Green function formalism which has been very useful in the treatment of ionization processes [42]. The advantage of this technique is that it can predict the energy position and relative strength of the satellite lines.

There is always a fundamental question concerning the validity of comparing a calculation for a three atom cluster Ni–N₂ with data for N₂ adsorbed onto a semi-infinite solid. The matrix isolation data of Klotzbucher and Ozin

Table 2
Relative binding energies of Ni–N₂ complexes

System	I ($5\sigma-1\pi$) _{coord} – ($5\sigma-1\pi$) _{gas} (eV)	II ($4\sigma-1\pi$) _{coord} – ($4\sigma-1\pi$) _{gas} (eV)	III ($5\sigma-4\sigma$) _{coord} – ($5\sigma-4\sigma$) _{gas} (eV)
Experiment			
N ₂ on Ni(110)	+1.7	+2.2	–0.5
Theory NiN ₂			
Δ SCF–HF [10]	–0.43	+0.40	–0.83
X_α SCF [35]	+2.9	+2.4	0.5
SCF–MO–CNDO [15]	+1.4	+1.5	–0.1

[27] demonstrated that the bonding of NiN_2 was different from that of the saturated complex $Ni(N_2)_4$. The N–N (Ni–N) stretch energy was 258.8 meV (57.7 meV) for the NiN_2 complex and shifted to 296.4 meV (34.9 meV) for $Ni(N_2)_4$. The low value of the N–N stretch coupled with the high Ni–N stretch energy would indicate that the single N_2 complex has a stronger N_2 –Ni bond caused by metal d to N_2 2π back bonding which weakens the N_2 bond. Therefore, we would expect to see a larger 2π back bonding contribution to the bonding in the NiN_2 cluster than in the surface complex. It is also intuitively obvious that a single metal atom bound to a N_2 molecule will not be as efficient at screening the photoinduced hole states on the N_2 molecule as a semi-infinite metal would be. Experiments on multi-metal carbonyl complexes indicate that a single metal carbonyl like $W(CO)_6$ produces approximately 60% of relaxation seen in a core hole ionization of CO adsorbed onto a surface [34]. Theoretical calculations by Baerends [43] show that the five other CO molecules in a complex like $W(CO)_6$ also contribute to the screening of a core hole localized on one CO molecule. Therefore, we should expect that the calculations for NiN_2 will give something less than 50% of the screening shift seen in the experimental data.

The major objectives of the comparison shown in tables 1 and 2 are two fold. (1) To obtain a qualitative picture of the N_2 –metal bond and; (2) to compare different calculational schemes to see if there are significant differences. We have chosen to make this comparison by looking at the shift in the valence energy levels from gas phase N_2 to adsorbed N_2 . The reason is that several of the theoretical schemes (specifically HF) do not correctly predict the binding energies of the gas phase N_2 levels, but they may correctly predict the shift in the N_2 levels upon adsorption. This seems to be (to us) the only fair comparison, but Hermann and Bagus have argued that the HF scheme works better for NiN_2 than for N_2 , so that our way of comparison exaggerates the error in HF [10]. Finally, we should note that Hermann and Bagus have used an excited state configuration of NiN_2 , so that they obtain better screening [10]. We have not listed the results of this calculation in table 1 or 2, because it is impossible to compare the other calculations. It is an artificial problem that will be solved by using larger clusters.

Table 1 shows that both the HF and the X_α techniques underestimate the relaxation shift. For example, look at the column for the 1π level. The experimental shift in energy ($\Delta_{1\pi}$) is 4.2 eV, where the positive sign means that the 1π binding energy of adsorbed N_2 is less than that of gas phase N_2 . This is primarily a consequence of final state screening, i.e. relaxation. The X_α scheme calculates a shift of the 1π level of 1.4 eV, which according to our arguments in a previous paragraph is approximately what should be expected for a NiN_2 cluster. On the other hand the HF procedure produces a negative shift of ~ 1.0 eV. This is because there is a much larger initial state shift downward than relaxation shift upward in the HF calculation. The calculated relaxation shift is very small (0.5 eV) [10]. This same phenomena was observed in HF calcula-

tions of NiCO [10b]. The many body SCF-MO-CNDO [15] calculation overestimates the 1π shift compared to the X_α or to our qualitative expectations. The calculated 1π shift in this scheme is +3.5 eV, which is 80% of the observed shift. The Ni-N spacing reported for the HF calculation is longer than the equivalent spacing in the X_α or CNDO calculation. There is no indication from the reported shifts of the 1π level upon coordination in the HF calculation that a shorter bond length would produce a positive $\Delta_{1\pi}$. In fact, increasing the Ni-N bond length to 2.1 Å in the HF calculation caused $\Delta_{1\pi}$ to change to -0.7 eV.

All three calculations show that the N₂ 4σ state shifts to high binding energy with respect to the 1π state upon coordination. This is easier to see in table 2 where we have specifically compared the 5σ to 1π (4σ to 1π) energy spacing in gas phase and coordinated N₂. The experimental data shows that the 5σ drops in energy (away from the Fermi energy) by 1.7 eV with respect to the 1π , while the change in the 4σ is even larger (2.2 eV). Column II of table 2 shows that all three calculations predict that the 4σ - 1π energy spacing will increase. The HF predicts a small change of 0.4 eV while the X_α value of 2.4 eV is very close to the experimental value of 2.2 eV. In contrast to the 4σ behavior, the three calculations disagree upon the sign of the change for the 5σ . The HF theory predicts a negative change, while both the X_α and CNDO show positive changes in agreement with the data. Bagus and Hermann [10] would argue that the apparent discrepancy of the HF theory shown in table 2 is a consequence of our method of calculating shifts, i.e. comparing the gas phase N₂. They believe the HF calculation is much better for NiN₂ than for N₂. If this argument is correct, their theoretical separation of initial and final state shifts upon coordination of N₂ is incorrect. Finally, column II shows the change in the 5σ and 4σ spacing upon coordination. Experimentally, the energy spacing increases by 0.5 eV. The HF theory predicts this increase with approximately the correct magnitude. According to this theory, the increase is caused by ~0.6 eV larger relaxation energy for the 5σ than for the 4σ [10]. The X_α theory has the wrong sign for the change in the 5σ to 4σ spacing, which as we will see appears to be contradictory to the picture of the bonding emerging from the X_α calculations.

We can now discuss the nature of the Ni-N₂ bond predicted from the theoretical calculations. The major perturbation of the N₂ molecule by the presence of the metal atom is to mix the two N₂ σ states, $2\sigma_u$ and $3\sigma_g$, to form new chemisorbed σ states that will appear much more like the lone pair orbitals of CO (fig. 1). If we write the new σ orbital in terms of the gas phase N₂ and Ni orbitals then

$$|\tilde{4}\sigma\rangle = A_1 |2\sigma_u\rangle + A_2 |3\sigma_g\rangle + \sum_{j>3} A_j |\psi_j\rangle, \quad (3a)$$

$$|\tilde{5}\sigma\rangle = B_1 |2\sigma_u\rangle + B_2 |3\sigma_g\rangle + \sum_{j>3} B_j |\psi_j\rangle. \quad (3b)$$

The ψ_j 's represent the remaining N_2 and Ni orbitals required to form a complete basis. Fig. 1 shows that if the metal atom bonds to the left, then if A_1 and A_2 (B_1 and B_2) are both positive, the 4σ (5σ) will look like a lone pair pointing towards the metal. If A_1 and A_2 have opposite signs, the new orbital will look like a lone pair pointing away from the metal atom. Since the new 4σ and 5σ states must be orthogonal and presumably are primarily composed of the N_2 $2\sigma_u$ and $3\sigma_g$ orbitals, one will be a lone pair towards the metal and the other away from the metal. Table 3 shows the charge density associated with the Ni and each of the two Ni atoms as calculated by HF [10] and X_α [35]. The Mulliken population analysis is shown for the HF calculation, and the charge in the spheres around each atom is listed for the X_α calculation. The inner sphere encloses all three small spheres [35]. Both calculations show that the 5σ

Table 3
Charge distribution in NiN_2

(a) $Ni-N_a-N_b$ ^a, Hartree-Fock calculation

Hartree-Fock [10] orbital	Mulliken population		
	Ni	N_a	N_b
4σ	0.03	0.63	0.34
5σ	0.03	0.32	0.65
1σ	0.01	0.53	0.46
$3d\pi$	0.97	0.01	0.02
2π			

(b) $Ni-N_a-N_b$ ^b, X_α scattered wave calculation [35]

Orbital	Ni sphere $r = 1.58 \text{ \AA}$	N_a sphere $r = 0.74 \text{ \AA}$	N_b sphere $r = 0.74 \text{ \AA}$	Inner sphere $r = 2.63 \text{ \AA}$	Outer sphere
4σ	0.476	0.471	0.050		-0.002
5σ	0.035	0.086	0.669	0.100	0.102
1π	0.044	0.40	0.315	0.0227	0.012
Ni($d\pi$)	0.824	-0.27	0.086	0.052	0.011
2π	0.240	0.230	0.286	0.192	0.053

^a $d(Ni-N) = 2.00 \text{ \AA}$, $d(N-N) = 1.1 \text{ \AA}$.

^b $d(Ni-N) = 1.83 \text{ \AA}$, $d(N-N) = 1.1 \text{ \AA}$.

orbital is the lone pair away from the metal atom in contrast to CO where the 5σ is the lone pair towards the metal. The HF calculation puts 65% of the charge in this orbital on the far atom and the X_α calculation has >70% of the charge on the nitrogen atom farthest from the metal. Then, as expected, the $4\tilde{\sigma}$ is the lone pair on the N atom near the metal atom. The HF calculation has 63% of the charge of the $4\tilde{\sigma}$ orbital on the near N atom, and the X_α calculation only 47%. Notice that the $4\tilde{\sigma}$ and $5\tilde{\sigma}$ lone pair type orbitals on coordinates N_2 are localized on the opposite ends of the molecule compared to the same orbitals in NiCO.

Even though both calculation schemes produce qualitatively the same picture of the mixing of the N_2 $2\sigma_u$ and $3\sigma_g$ states to form the σ valence orbitals of NiN_2 , the nature of the bond seems to be quite different. The X_α calculation predicts that the σ state which forms a N_2 lone pair towards the metal, bonds to the metal. There is 48% of the charge for the $4\tilde{\sigma}$ orbital inside of the Ni sphere, while according to the HF theory only 3% of the charge is on the Ni atom. The $5\tilde{\sigma}$ orbital, which is the N_2 lone pair away from the metal, is more asymmetric with respect to N_2 in the X_α than in the HF calculation, while both predict little weight on the metal atom. The X_α theory also shows more d- 2π back bonding than the HF does. This can be seen in the HF $3d\pi$ and $X_\alpha Ni(d\pi)$ levels. There is only 3% of this orbital on the N_2 molecule in the HF calculation, while the X_α calculation shows $\sim 11\%$ of this level to be as 2π on the N_2 . We pointed out previously that the 2π character in NiN_2 should be larger than in a saturated system like $Ni(N_2)_4$ or adsorbed N_2 . Notice that both calculations show very little distortion of the 1π level, justifying our use of this level as a reference in table 2.

Table 3 shows quite clearly that there is still a large difference between the HF and X_α results for the nitrogen-Ni bond. There are several other theoretical calculations that need to be done before the correct picture of the N_2 metal bond can be determined. First larger clusters should be investigated, either saturated configurations like $Ni(N_2)_4$ or multimetal clusters like $(Ni)_5N_2$, so that the screening will be come more realistic and a single N_2 -metal bond may be more similar to the surface situation. Second, local density calculations need to be done without the use of muffin tins. The choice of the sphere radii does effect the binding energies especially of levels like the 1π and 2π which have considerable charge in the inner sphere region. Finally, as difficult as it is, it would be very informative to go beyond HF theory, so that some correlation can be included.

There is a fundamental question about the validity of the single particle calculation to reproduce the measured binding energies when satellite or shake-up lines are observed. These lines are due to electron-electron interaction and their position and intensity effects the main line intensity and position [41,45]. If a theoretical calculation scheme can not accurately predict the satellite line positions and intensities then it is questionable that the same theory can be trusted to calculate the main line position. The signs of this many-body effect

in any self-consistent field calculation are quite easy to see. If the charge distribution in specific single particle orbitals changes dramatically between the neutral ground state calculation and the single hole ionic calculation, then shake-up or satellite lines will be important. Hermann and Bagus [10] showed that there is a large charge reorganization or redistribution upon creating a $5\tilde{\sigma}$ hole in the NiN_2 molecule. If we consider only the valence N_2 orbitals ($3\tilde{\sigma}$, $4\tilde{\sigma}$, $1\tilde{\pi}$ and $5\tilde{\sigma}$) then 50.6% of the charge on the neutral N_2 molecule is on the nitrogen near the metal. When a $5\tilde{\sigma}$ hole is created, the fraction of the charge on the nearest N atom does not change much (50.7%), but the individual orbital character is quite different. The neutral 5σ orbital only had 65% of its charge on the outer N atom, but the $5\tilde{\sigma}$ hole state has a single electron with 90% of its weight on the outer N atom [10]. The doubly occupied $4\tilde{\sigma}$ level has 63% of its weight on the nearest N atom in the neutral and 87% in the 5σ hole state [10]. The ionic state accentuates the asymmetry of the σ states. The many-body Green function calculation for NiN_2 predicts that 40 to 50% of the intensity is lost from the main line into satellite lines for the $4\tilde{\sigma}$ and $5\tilde{\sigma}$ levels [15]. A clear sign of the many-body effects in the theory is the apparent wrong sign of the shift in the near core $3\tilde{\sigma}$ level shown for the SCF-MO-CNDO calculation in table 1. The theory predicts that considerable intensity is "stolen" from the N_2 3σ level upon coordination. The new satellite lines appear at lower binding energy than the original 3σ level. A consequence is that the "main line" moves to high binding energy and loses intensity. We were unable to clearly identify a 3σ level in these measurements.

4.2. Multi-electron excitations (shake-up)

Satellite lines are an integral part of the photoionization process from any system where the electrons interact. This means that satellite lines will be seen in the photoionization from all systems except single electron systems like atomic H. The easiest way to picture the origin of these lines is in the sudden approximation. Here we visualize that the removal of the electron by adsorption of the photon is so sudden that all of the $N-1$ electrons remaining are "frozen" in their neutral state configuration. Since the $N-1$ electrons interact with the hole state caused by ionization, this frozen neutral configuration is not an eigenstate of the ionic system. The projection of this artificial frozen ionic state onto the real $N-1$ ionic states of the system will give the relative intensities of the multiple lines seen in the photoionization process [45]. A couple of simple examples will suffice to explain this phenomena. Consider photoionization from the 1σ level of N_2 (the N_{1s} electron). If there is no rearrangement of charge after the hole is created, then the neutral and ionic states will be the same and all of the intensity is contained in one line corresponding to the ionic configuration $1\sigma^1 2\sigma^2 3\sigma^2 4\sigma^2 1\pi^4 5\sigma^2$. In this non-interacting case, the binding energy is given by Koopmans' theorem. It is the HF orbital energy, which is ~ 427 eV [46]. Experimentally, the binding energy

for the N_{1s} electron in N_2 is $\sim 410\text{eV}$ [47], which means that there is approximately 17 eV lowering of the total energy of the ionic state by reorganization of the $N - 1$ electrons in the presence of the hole. The projection of this relaxed ionic state onto the frozen orbital ionic state is not one to one, so that the remaining intensity is "borrowed" by other ionic configurations [41,45]. One of the new configurations with the most intensity is a 2-hole, 1-particle state with the configuration $1\sigma^1 2\sigma^2 3\sigma^2 4\sigma^2 1\pi^3 5\sigma^2 1\pi^1$, i.e. a 1π to 2π shake-up on the N_{1s} ionization. The energy of this ionic configuration is ~ 15 eV higher than that of the single 1σ hole state.

Manne and Aberg [45] theoretically proved that there is a sum rule on the intensity and on the first moment of the energy of the lines associated with the ionization of a core level. The sum of the intensities of all the satellite lines is equal to the single particle photoionization cross section, so the satellite lines borrow intensity from the main line. The sum of the intensity weighted energies of all of the lines is equal to the HF orbital energy or Koopmans' value [45]. This means that the intensity and energy position of the main line are dependent upon the energy and intensity of the satellite lines. Freund et al. [41] have experimentally shown that these two sum rules are obeyed for diatomic molecules and $\text{Fe}(\text{CO})_5$.

When N_2 or CO is coordinated to a metal atom or atoms, the intensity and number of satellite lines in the core level spectra increases compared to the gas phase molecule [9,16,34,41]. The sum rule requires that the number or intensity of the satellite lines increase to offset the ~ 5 eV shift of the main line to lower binding energy. Experiments on $\text{Fe}(\text{CO})_5$ show that the O_{1s} main line has lost 28% of its intensity compared to CO. Almost all of this intensity went into a new (compared to CO) satellite line at approximately 6 eV higher binding energy than the main line [41]. This new satellite line is characteristic of the core level spectra of all coordinated complexes of N_2 and CO [9,16,34,41]. It originates from an excitation from the bonding to non-bonding 2π -metal orbitals in the coordinated complex [48]. When the core hole is created in the ligand, the charge from the metal atom flows towards the ligand to screen the hole. This screening charge occupies the metal- 2π orbital of the ion [49] making the bonding metal- 2π orbital mostly 2π in character [44]. The antibonding metal- 2π orbital is now mostly metal in character, so that an excitation from the bonding to the anti-bonding 2π -metal orbital is a charge transfer excitation. This leads to the common notation that the two major peaks in the core level spectra of coordinated N_2 or CO are due to the "screened" and "unscreened" final states [9,48]. Obviously, the energy separation between the bonding and anti-bonding 2π -metal d energy levels depends upon the interaction energy between the molecule and metal. The energy separation for CO on Cu(100) with a heat of adsorption of ~ 0.6 eV is ~ 2 eV, while more strongly chemisorbed CO on W(110) exhibits a 2π -metal (bonding) to 2π -metal (anti-bonding) transition in the ion of ~ 6 eV [16].

The arguments presented in the previous paragraphs for core level photoioni-

zation should also be relevant to valence level ionization. The problem is that the density of levels in this region make identification and assignment of satellite lines much more difficult than in a core level spectrum. For example, if you knew that a satellite line near the N_{1s} ionization potential corresponded to a ionic configuration $1\sigma^1 2\sigma^2 3\sigma^2 4\sigma^2 1\pi^3 5\sigma^2 2\pi^1$, you would immediately call this line a 1π to 2π shake-up line off of the N_{1s} main line. But if you knew that a satellite line in a valence spectrum corresponded to a configuration $1\sigma^2 2\sigma^2 3\sigma^2 4\sigma^2 1\pi^3 5\sigma^1 2\pi^1$, you could call it a satellite line of the 5σ or 1π ionization. This implies that the identification and labeling of satellite lines in the valence region of the spectra can only be done with the aid of a theoretical calculation. There have been very few calculations of the many-body valence spectra of coordinated molecules [15].

It has been recognized for some time that there are many-body satellite lines in the gas phase valence spectra of molecules like N_2 and CO [42]. We show in fig. 10 a comparison of photoelectron spectra of physisorbed N_2 on Pd(111) and the gas phase spectrum of N_2 [47]. There are several small peaks between the 3σ and 4σ single particle peaks. A calculation by Schirmer et al. [42] identified these many-body satellite lines. The peak at -19.5 eV (our scale) is a shake-up from the $4\sigma(2\sigma_u)$ level. The peak at -21 eV (fig. 10) is a shake-down from the $3\sigma(2\sigma_g)$ level. This is caused by having a 2-hole, 1-particle ionic state lower in energy than the single hole state. The third peak is a combination of a shake-up peak from the 4σ and a shake-down on the 3σ . Given the fact that the photon energies and collection geometries are different for the gas phase and condensed N_2 spectra in fig. 10, they show the same qualitative many electron excitations. This should be expected, since we have not perturbed the energy level scheme. The only multi-electron excitation that should be quite different in condensed N_2 compared to gas phase N_2 are those

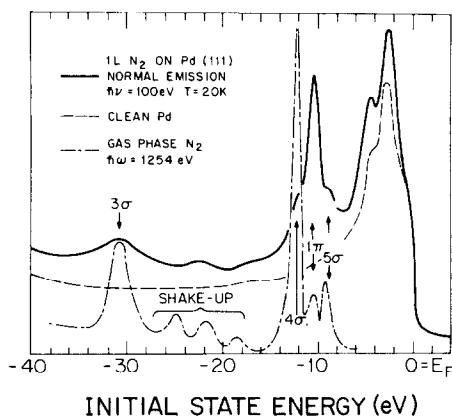


Fig. 10. Photoelectron spectrum of N_2 adsorbed on Pd(111) at 20 K ($\hbar\omega < 100$ eV) compared to clean Pd and gas phase N_2 at $\hbar\omega = 1254$ eV [46].

leaving one electron in a high lying Rydberg state. These Rydberg states will probably be smeared out in the condensed layer [41].

The multi-electron excitations in chemisorbed N₂ should be quite different from those in condensed or gas phase N₂. The N₂ chemically bonds to the substrate forming new occupied and unoccupied energy levels. The binding energy of the valence levels of N₂ are shifted to lower binding energy by ~4 eV due to the screening of the photoinduced hole by the metal electrons. This shift must be compensated by borrowing intensity from the main line and putting this intensity into higher binding energy satellite lines. An analysis of the core level spectra of N₂ on Ni(100) shows that the 2π-metal bonding and anti-bonding levels are separated by ~5 eV [9].

In fig. 11, we have compared our normal emission photoelectron spectrum for N₂ adsorbed on Ni(110) with the many-body calculation of Saddei et al. [15]. This theory does not calculate the cross section, and it does not reproduce the experimental binding energies of N₂ or chemisorbed N₂ correctly. Therefore, we have adjusted the calculated values in the following manner.

- (1) The chemisorbed 1π level was used as the reference level. The theoretical 1π level was shifted to appear at -7.8 eV energy in fig. 11.
- (2) All of the theoretical values were referred to the experimental N₂ ionization potentials. For example table 3 shows that the 5σ to 1π spacing in the coordinated N₂ is 1.4 eV larger than gas phase N₂. Using the experimental values for gas phase N₂ gives (5σ - 1π)_{corr} = 0.0 eV. The same procedure gives (4σ - 1π)_{corr} = 3.3 eV.
- (3) The main line intensities were adjusted to correspond to the experimental

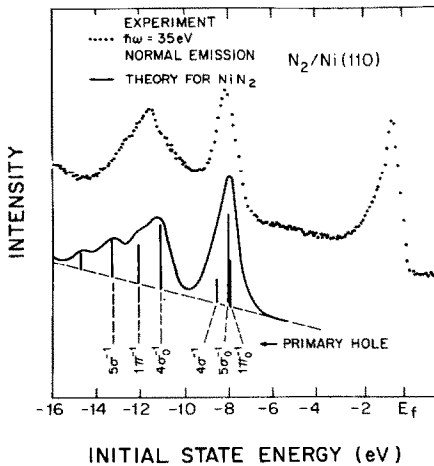


Fig. 11. Comparison of normal emission photoelectron spectrum of N₂ adsorbed on Ni(110) with many-body calculation of Saddei et al. [15]. The notation at the bottom indicates the primary hole configuration. A subscript 0 indicates the main line.

intensity. The relative satellite line intensity is calculated [15].

(4) Each discrete line is broadened into a ~ 1.1 eV Gaussian corresponding to the line width observed on the 5σ level.

The main lines are by definition in this calculation the lines with the highest intensity. They are marked by a subscript 0 in fig. 11. All of the other satellite lines involve charge transfer excitations of the form discussed previously, i.e. metal- 2π bonding to the metal- 2π anti-bonding. The energies of the intense satellite lines are in the range of 4.5 to 7 eV, which is in qualitative agreement with the N_{1s} core level satellite at 5 eV. This figure should not be interpreted as a quantitative explanation of the experimental data, but instead as a qualitative picture of the effect of many-body excitations on the valence photoemission spectra of weakly chemisorbed N_2 .

Using the theoretical assignment given in fig. 11, we can offer a qualitative explanation for the photon energy dependence of the spectra shown in figs. 6, 8 and 9. At low photon energies, the branching ratios for gas phase N_2 show that the 1π level dominates the total cross section [17]. Therefore, the 1π shake-up lines below the 4σ main line become the dominant peaks, causing the center of the broad -12 eV peak to shift to higher binding energy. As the photon energy increases the σ states become more intense, shifting the peak center to lower binding energy. There are two criticisms of this argument. First the gas phase cross sections will not account for the variations in cross section for angle resolved detection from a molecule with fixed orientation [18]. In addition, the angular dependence of the satellite lines is unknown. A second complication is due to the transition from the energy region where the sudden approximation is valid to the low energies where the adiabatic limit is reached. Experiments on the valence shake-up in single metal carbonyls indicate that this transition region is within 10 eV of threshold [50]. The data shown in fig. 9 range in kinetic energy from ~ 6 to ~ 24 eV.

The explanation of the satellite line structure in the photoemission spectra of adsorbed N_2 would indicate that this type of structure should be seen in the spectra from any N_2 or CO complex. The observation of satellite lines in the photoemission spectra of chemisorbed CO is rare, with the CO on Cu system being the only clear example [39]. The general conclusion seems to be that valence band shake-up can be seen on weakly chemisorbed systems like CO on Cu (0.6 eV binding energy) or N_2 on Ni (0.4 eV binding energy), but when the binding energy increases to greater than 1 eV for strong chemisorption or to very small numbers for physisorption, no clear valence satellite structure is seen. The explanation for the physisorption is obvious [44], but the lack of structure in the strong chemisorption case is, contradictory. There is a large relaxation shift which must be accompanied by intensity borrowing by satellite lines. The reason that well defined satellite lines are not observed is not because they are missing but a result of spreading the intensity over a large energy range. The first effect of strong substrate ligand coupling is to increase the energy of the metal- 2π bonding to anti-bonding transition [16]. If the

shake-up is higher in energy, then less intensity has to be transferred to the satellite line to conserve the energy sum rule [41]. In addition, strong coupling with a metallic substrate implies that the discrete molecular orbitals of the metal surface complex will be broadened into resonances causing the satellite line intensity to be spread over a wide energy range.

5. Conclusions

We have investigated the N_2 -Ni bond using angle resolved photoelectron spectroscopy and inelastic electron scattering. The experimental data indicate that N_2 bonds to a single Ni atom with its axis perpendicular to the surface on Ni(110). Comparison of the data to theoretical calculations of the NiN_2 complex shows that bonding is primarily through a N_2 4σ -metal bond with a small amount of Ni d- N_2 2π back bonding. The chemisorbed N_2 molecule has lost the inversion symmetry of the homopolar N_2 molecule. This loss of inversion symmetry is seen in the data through: (1) the infrared active N-N stretch mode with an $e^* \gtrsim 0.45e$; (2) a very intense Ni- N_2 stretch mode with an $e^* \gtrsim 0.31e$, approximately three times larger than the corresponding Ni-CO mode; (3) the mixing of the N_2 $2\sigma_u$ and $3\sigma_g$ states to form lone pairs like σ states of chemisorbed N_2 ; and the presence of a final state resonance in the photoionization cross section of the 4σ level of adsorbed n_2 . The N $2\sigma_u$ level from which the chemisorbed 4σ level originates does not display a final state resonance in the photoionization cross section because it is forbidden by symmetry rules.

The valence band spectra of chemisorbed N_2 contains many satellite lines due to interaction of the surface complex with the photoinduced hole. A Green function many-body calculation for NiN_2 gives a qualitative description of this valence spectrum.

Acknowledgements

We would like to thank the staff at the Synchrotron Radiation Center, University of Wisconsin-Madison, for their support. One of us (K.H.) would like to thank the Deutsche Forschungsgemeinschaft for a travel grant. The inelastic electron scattering work was supported by NSF under Grant No. DMR-78-08520. The angle resolved photoelectron spectroscopy was supported by the Material Research Laboratory of the University of Pennsylvania under the NSF grant No. DMR-79-23647.

References

- [1] J.C. Fuggle and D. Menzel, in: Proc. 7th Intern. Vacuum Congr. and 3rd Intern. Conf. on Solid Surfaces, Vienna, 1977, p. 1003.
- [2] J.C. Fuggle and D. Menzel, *Vakuum-Tech.* 27 (1978) 130.
- [3] E. Umbach, A. Schichl and D. Menzel, *Solid State Commun.* 36 (1980) 93.
- [4] M. Goltze, W. Hirschwald, M. Grunze and B. Driscoll, to be published.
- [5] P.S. Bagus, C.R. Brundle, K. Hermann and D. Menzel, *J. Electron. Spectrosc. Related Phenomena* 20 (1980) 253.
- [6] W. Ho, R.F. Willis and E.W. Plummer, *Surface Sci.* 95 (1980) 171.
- [7] M. Grunze, R.K. Driscoll, G.N. Burland, J.C.L. Gornish and J. Pritchard, *Surface Sci.* 89 (1979) 381.
- [8] R.A. Shigeishi and D.A. King, *Surface Sci.* 62 (1977) 379.
- [9] K. Hermann and P.S. Bagus, *Solid State Commun.* 38 (1981) 1257.
- [10] (a) K. Hermann, P.S. Bagus, C.R. Brundle and P. Menzel, to be published;
(b) P.S. Bagus, K. Hermann and M. Seel, *J. Vacuum Sci. Technol.* 18 (1981) 435.
- [11] J.B. Johnson and W.G. Klemperer, *J. Am. Chem. Soc.* 99 (1977) 7132.
- [12] D.R. Salahub, private communication.
- [13] K. Hermann and P.S. Bagus, *Phys. Rev.* 16 (1977) 4195.
- [14] D.E. Ellis, E.J. Baerends, H. Adachi and F.W. Averill, *Surface Sci.* 95 (1980) 477.
- [15] D. Saddle, H.J. Freund and G. Hohlneicher, *Surface Sci.* 95 (1980) 527.
- [16] J.C. Fuggle, E. Umbach, D. Menzel, K. Wandelt and C.R. Brundle, *Solid State Commun.* 27 (1978) 65.
- [17] E.W. Plummer, T. Gustafsson, W. Gudat and D.E. Eastman, *Phys. Rev.* A15 (1977) 2339.
- [18] J.W. Davenport, *Phys. Rev. Letters* 36 (1976) 945.
- [19] C.L. Allyn, T. Gustafsson and E.W. Plummer, *Solid State Commun.* 28 (1978) 85.
- [20] G. Loubriel and E.W. Plummer, *Chem. Phys. Letters* 64 (1979) 234.
- [21] C.T. Allyn, T. Gustafsson and E.W. Plummer, *Rev. Sci. Instr.* 49 (1978) 1197.
- [22] B. Tonner, *Nucl. Instr. Methods* 172 (1980) 133.
- [23] M. Nistijima, S. Masuda, Y. Sakisaka and M. Onchi, *Surface Sci.* 107 (1981) 31.
- [24] F.A. Cotton and G. Wilkinson, *Advanced Inorganic Chemistry* (Interscience, 1972);
L.H. Jones, R.S. McDowell and M. Goldblatt, *J. Chem. Phys.* 48 (1968) 2663.
- [25] B. Flokesson, *Acta Chem. Scand.* 26 (1972) 4008.
- [26] L.J. Bellamy, *The Infrared Spectra of Complex Molecules*, 3rd ed. (Chapman and Hall, London, 1975).
- [27] W. Klotzbucher and G.A. Ozin, *J. Am. Chem. Soc.* 97 (1975) 2672.
- [28] The effective charge e^* is a measure of the magnitude of the dynamic dipole; for example, see H. Ibach, *Surface Sci.* 66 (1977) 56.
- [29] S. Andersson and J. Davenport, *Solid State Commun.* 28 (1978) 677.
- [30] The first measurement of this type was made by Smith et al. [31], the existing data are tabulated in ref. [32].
- [31] R.J. Smith, J. Andersson and C.J. Lapeyre, *Phys. Rev. Letters* 37 (1976) 1081.
- [32] E.W. Plummer and W. Eberhardt, *Angle Resolved Photoemission as a Tool for the Study of Surfaces*, in: *Advances in Chemical Physics*.
- [33] K. Horn, A.M. Bradshaw and K. Jacobi, *Surface sci.* 72 (1978) 719;
K. Horn, A.M. Bradshaw; K. Hermann and I.P. Batra, *Solid State Commun.* 21 (1977) 75.
- [34] E.W. Plummer, W.R. Salaneck and J.S. Miller, *Phys. Rev.* B18 (1978) 1673.
- [35] F. Pinski and R. Messmer, private communication.
- [36] B.G. Baker, B.B. Johnson and G.L.C. Maire, *Surface Sci.* 24 (1971) 572.
- [37] J.E. Demuth, *Surface Sci.* 65 (1977) 369.
- [38] T.N. Taylor and P.J. Estrup, *J. Vacuum Sci. Technol.* 10 (1973) 26.
- [39] P.R. Norton and R.L. Tapping, *Chem. Phys. Letters* 38 (1976) 207;
C.R. Brundle, *J. Electron. Spectrosc. Related Phenomena* 7 (1975) 484.

- [40] P.R. Norton, R.L. Tapping, H.P. Broida, J.W. Gadzuk and B.J. Wacławski, Chem. Phys. Letters 53 (1978) 465.
- [41] H.-J. Freund, E.W. Plummer, W.R. Salaneck and R.W. Bigelow, J. Chem. Phys. 75 (1981) 4275.
- [42] J. Schirmer, L.S. Cederbaum, W. Domcke and W. von Niessen, Chem. Phys. 26 (1977) 149.
- [43] E.-J. Baerends calculated the charge redistribution in $Cr(CO)_6$ due to a C_{1s} hole in one CO molecule, see ref. [44] for the figure.
- [44] H.-J. Freund and E.W. Plummer, Phys. Rev. B23 (1981) 4859.
- [45] R. Manne and T. Aberg, Chem. Phys. Letters 7 (1962) 282.
- [46] J. Müller, H. Agren and O. Goscinski, Chem. Phys. 38 (1979) 349.
- [47] K. Siegbahn, C. Nordling, G. Johansson, J. Hodman, P.F. Hodin, K. Hamrin, U. Gelius, T. Bergmark, L.O. Werme, R. Manne and Y. Baer, ESCA Applied to Free Molecules (North-Holland, Amsterdam, 1969).
- [48] K. Schönhammer and O. Gunnarsson, Solid State Commun. 23 (1971) 691; O. Gunnarsson and K. Schönhammer, Phys. Rev. Letters 41 (1978) 1608.
- [49] N.D. Lang and A.R. Williams, Phys. Rev. B16 (1977) 2408.
- [50] D.S. Rajoria, L. Kounat, E.W. Plummer and W.R. Salaneck, Chem. Phys. Letters 49 (1977) 64.